ICAS-88-2.2.1

TRANSONIC INVESTIGATIONS ON HIGH ASPECT RATIO FORWARD- AND AFT-SWEPT WINGS

Takeshi OHNUKI and Nobuhiko KAMIYA
National Aerospace Laboratory
7-44-1 Jindaijihigashi-Machi, Chofu, Tokyo, 182, JAPAN

ABSTRACT

An experimental investigation has been carried out to study the effect of sweep angle change on the performance of wing-fuselage configurations. This paper discusses the fundamental aerodynamic characteristics of forward-swept wings in detail.

This wing model has no twist and has the same symmetrical airfoil sections at every spanwise section. It is a half model and can be set as forward-, non-, and aft-swept configurations. The sweep angle of 40% chord line ranges from -15° up to $+15^{\circ}$.

Lift, drag, and pitching moment are measured at Mach number ranging from 0.7 to 0.85 using a 3-component strain gauge balance. And wakes of the wing are surveyed simultaneously. Reynolds number based on its mean aerodynamic chord is about 1.0×10^6. Tests are conducted in 2M x 2M Transonic Wind Tunnel of National Aerospace Laboratory.

It is concluded that the forward-swept wing has the fundamental characteristics such as smaller wave drag, cleaner boundary layer, and larger induced drag than a structurally equivalent aft-swept wing. And one of the problems that should be solved is the strong shock wave at inner-wing portion.

1. INTRODUCTION

Since Krone[1] showed that the hurdle for the forward-swept wing (FSW) could be overcome by the technique of aeroelastic tailoring of composite materials, FSW has appeared on the stage again. Several aerodynamic potential of FSW has been shown, that is, FSW may provide extended lateral controllability at high attack angles[2], better low-speed handling qualities[3], and reduced transonic maneuver drag[3]. Many of the works, therefore, concern fighter aircrafts which are demanded a good maneuverability. On the contrary, there are fewer works and less experience on designing high aspect-ratio FSW for transport aircrafts. Because high cruise efficiency to minimize fuel consumption is called for transports, there exist differences between fighter and transport design concepts.

According to Ref. 4, FSW without twist has its maximum local lift coefficient inboard at high angles of attack and the flow separates at the center first. And compared with ASW under the constraints of 1) optimised twist to ensure elliptic load distribution at C_L=0.45 and 2) that the onset of flow separation is inboard at C_L=1.0, FSW of the same aspect ratio has lower induced drag. As Munk[5] showed that induced drag depends on only spanwise distribution of circulation but not on its streamwise position, induced drag, therefore, is usually obtained by calculation in the Trefftz plane. One of the clearest distinctions between FSW and ASW, however, is the streamwise location of the edge of trailing vortices. A simple calculation in near field indicates that the downwash of FSW is stronger than that of ASW of the same distribution of circulation. As induced drag is approximately proportional to induced velocity, FSW has larger induced drag than ASW. (This will be discussed later in 3. RESULTS AND DISCUSSIONS.) This simple analysis indicates that the strength of downwash depends on also streamwise location of circulation and this means that induced drag of FSW is fundamentally large.

The purpose of this paper is to shed light on the fundamental aerodynamic characteristics of a high aspect-ratio forward-swept wing with fuselage in transonic flow.

2. MODELS AND TESTS

The wing model has no twist and same symmetrical airfoil sections at every spanwise station. This is a half model and has about 400 mm half span. The wing is set as forward-, non-, and aft-swept configurations changing its sweep angle. The sweep angle of 40% chord line ranges from -15° up to $+15^{\circ}$. The planforms are shown in Fig. 1. The wing tip of each configuration is adjusted to keep constant aspect ratio of 9.5. Therefore wing areas and taper ratios slightly differ from the values of the non-swept wing (NSW) configuration. Leading particulars are summarized in Table 1. When the sweep angles of 40% chord line of FSW and ASW are equal, we can generally assume that they are structurally equivalent since 40% chord line is approximately the center of the box structure of conventional transport. In this paper, therefore, the sweep angle is defined as the angle between

CONFIG.	SWEEP ANGLE (DEG.)	ASPECT RATIO	TAPER RATIO	HALF SPAN (mm)	WING AREA (mm^2)	MAC (mm)
FSW	-15	9.5	0.262	407	3.5×10^4	95.7
NSW	0	9.5	0.3	400	3.4×10^4	92.4
ASW	+15	9.5	0.273	401	3.4×10^4	93.7

Table 1. Leading particulars

40% chord line of the wing model and the line perpendicular to the uniform flow.

The airfoil of this model, which was designed so that the flow could be accelerated up to about 55% chord at Mach number 0.8, is symmetrical and of 12% maximum thickness/chord ratio (Fig. 2). The specific pressure distribution was determined considering natural laminar flow.

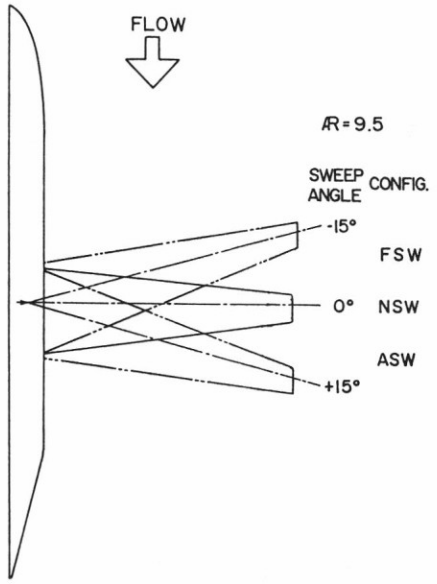

Fig. 1. Tested Configurations

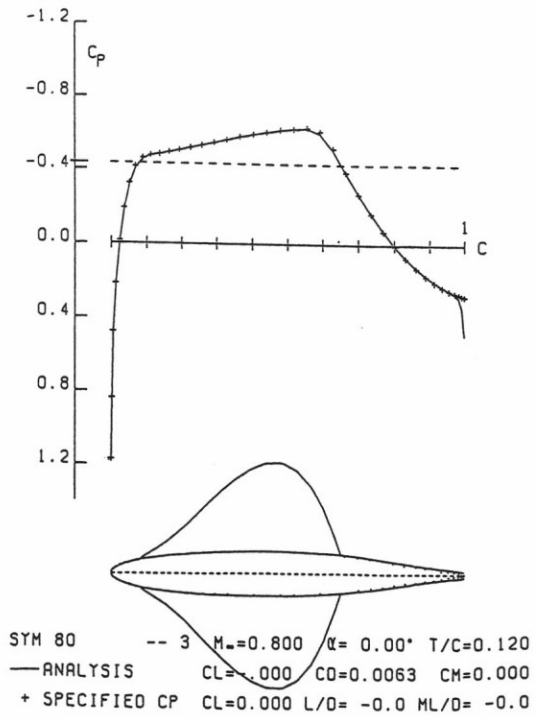

Fig. 2. Airfoil And Calculated Pressure Distribution

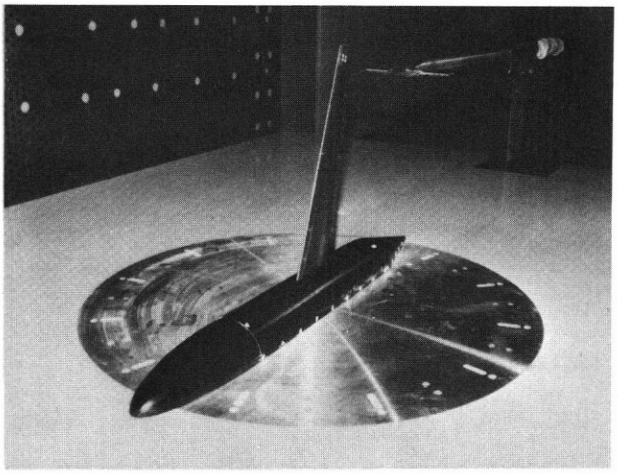

Fig. 3. Wund Tunnel Test Setup

The wing model is mounted on an axisymmetric half-body with elliptic nose and conical afterbody.

Tests are conducted in 2M x 2M Transonic Wind Tunnel of National Aerospace Laboratory. A reflection plate is set on the floor of the test section and the models are set on it (Fig. 3). The boundary layer along the plate is about 16 mm thick at the center of balance.

Lift, drag, and pitching moment are measured at Mach number ranging from 0.7 to 0.85 using a 3-component strain gauge balance and wakes of the wing are surveyed simultaneously. Reynolds number based on its mean aerodynamic chord is about 1.0 x 10^6.

3. RESULTS AND DISCUSSIONS

3-1 ON DESIGNED CONDITION -- DRAG AT ZERO LIFT

Drag polar curves at several Mach numbers are shown in Fig. 4. The data of fuselage was subtracted from that of wing-fuselage configurations. Drag coefficients of FSW at zero lift are smaller than those of ASW. Comparison between experimental and analyzed pressure distributions at Much number of 0.7 and attack

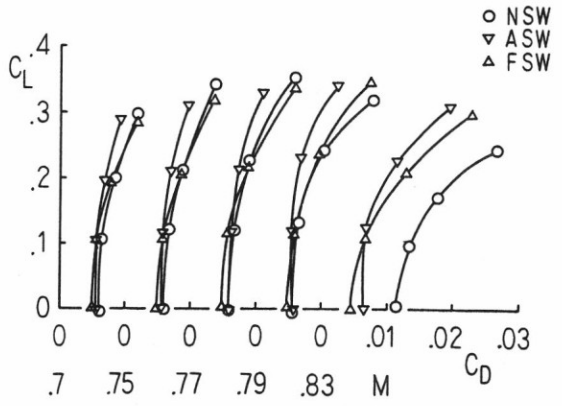

Fig. 4. Drag Polar Curves

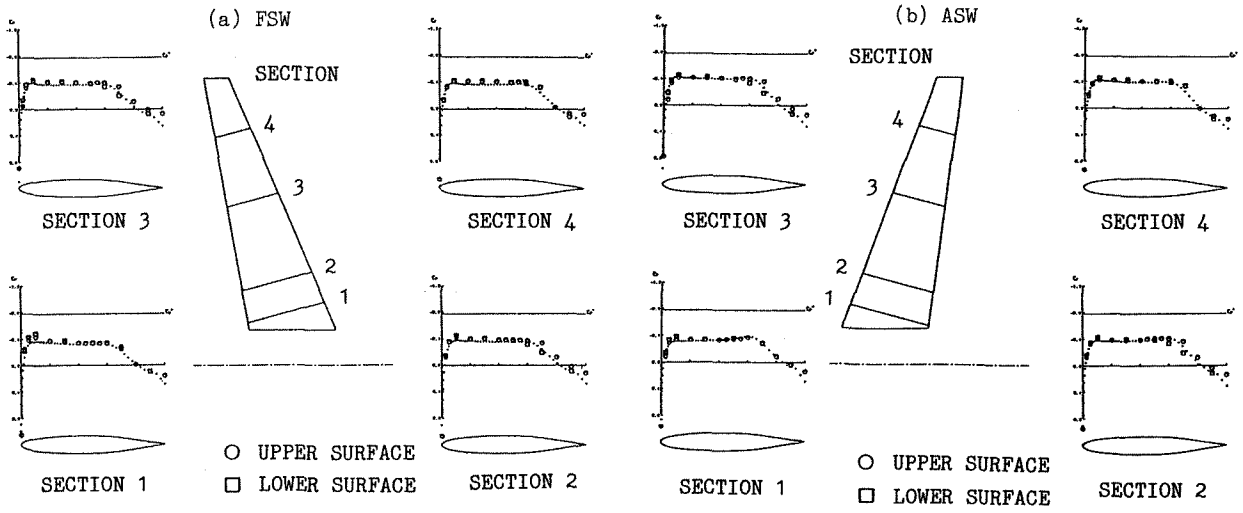

Fig. 5. Comparison between Experiments And Numerical Analyses
(Mach number = 0.7, attack angle = 0°)
○ □ Experiments
····· Calcurated

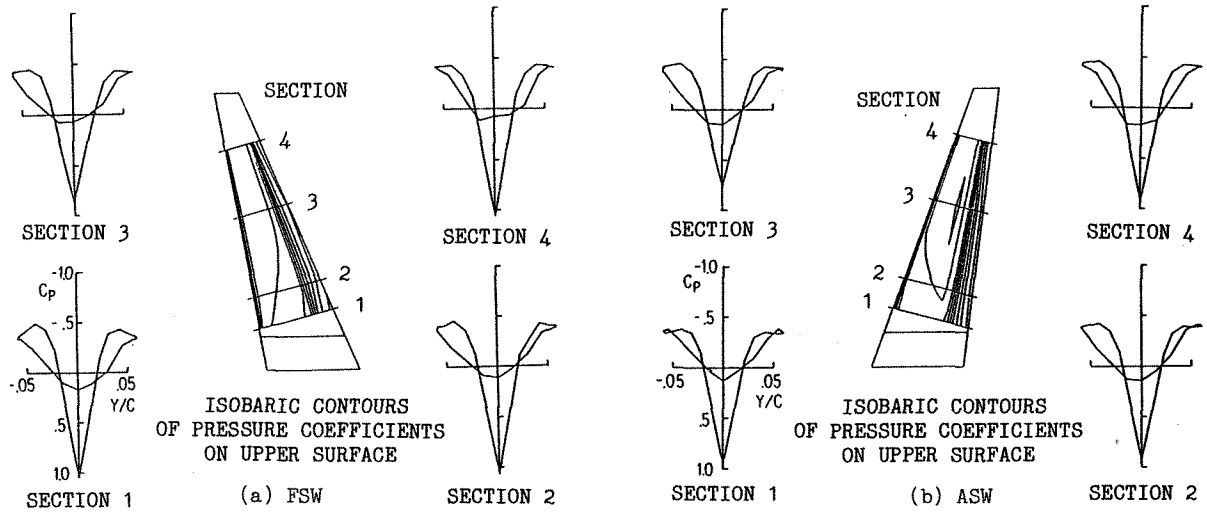

Fig. 6. Pressure Distributions at Four Sections And
Isobaric Contours of Pressure Coefficients on Upper Surface
(Mach number = 0.7, attack angle = 0°)

angle of 0° is shown in Fig. 5. In this analysis, full potential code called "YOKUDO-P" was used[6]. That is one of NAL's analysis codes for wing-fuselage configurations. The agreement is fairy good except at the root of FSW where the analyses underestimated the suction peak. Measured pressure distributions along the axis perpendicular to the flow are plotted in Fig. 6 to analyze the pressure drag. FSW has bigger thrust loop at the root than ASW because of the suction peak before the crest point. Compared with this difference of pressure drag, the experimental value of the drag of FSW is too much smaller. Then we are forced to arrive at a conclusion that this difference is resulted from viscous effects. As Paisley et al[7] suggested, the boundary layer on FSW may be laminar in a much larger region than that on ASW because the leading-edge sweep of FSW is smaller and FSW is not likely to affected by the boundary layer along the fuselage.

As for drag divergence Mach number (M_{DD}), M_{DD} of FSW is greater at low lift coefficients (Fig. 7). M_{DD} at zero lift of FSW, ASW, NSW (non-swept wing) are 0.830, 0.825, 0.804, respectively. Under the condition of attack angle 0° and Mach number 0.83, which is on M_{DD} for FSW and just beyond for ASW, shock waves exist only on outboard for both FSW and ASW (Fig. 8). Shock sweep of FSW

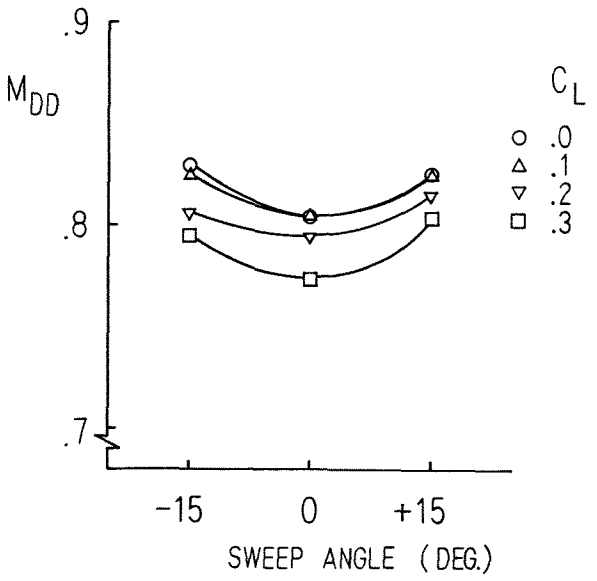

Fig. 7. Drag Divergence Mach Numbers for Each Configuration

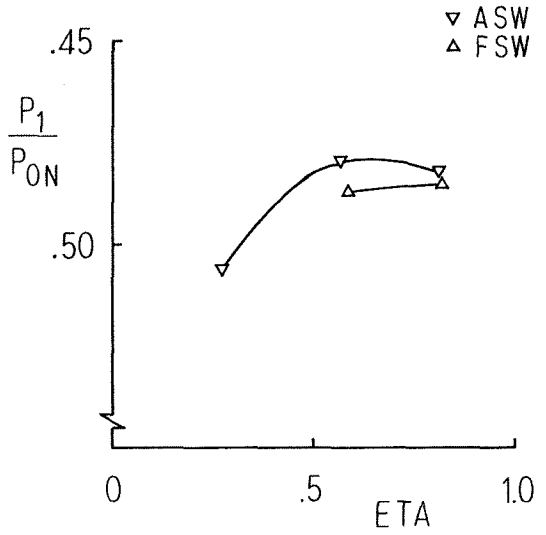

Fig. 9. Spanwise Distributions of P_1/P_{ON}

P_1 : Static Pressure Just Upstream of Shock Wave

P_{ON}: Total Pressure for The Flow Normal to The Direction of Shock Sweep

(Mach number = 0.83, attack angle = 0°)

is 18.5° and much higher than 9.4° of ASW. Fig. 9 shows spanwise distributions of P_1/P_{ON}, where P_1 is static pressure just upstream of the shock wave and P_{ON} is total pressure for the flow normal to the direction of shock sweep. This figure also indicates the spanwise distribution of the strength of shock wave and therefore the amount of wave drags. Shock wave of FSW is weaker than that of ASW in spite of the fact that the pressure upstream of the shock wave at each section is almost the same through all configurations, and disappears at inner- and mid-span. This fact indicates that firstly M_{DD} of FSW is higher than that of ASW and secondly the drag divergence occurs due to the outboard shock wave for both FSW and ASW.

3-2 OFF DESIGNED CONDITION

Suppose a vortex was placed as shown in Fig. 10, and the spanwise distribution of circulation kept constant in spite of the sweep angle change. Calculated induced drag is plotted in Fig. 10 as a function of sweep angle. The value of drag is non-dimensionalized by that of NSW. In this comparison induced drag of FSW is much larger than that of ASW. In case of sweep angle of 15°, for example, the induced drag of FSW is about 1.3 times greater than that of ASW. Indeed it is not worth making quantitative discussions under these simple

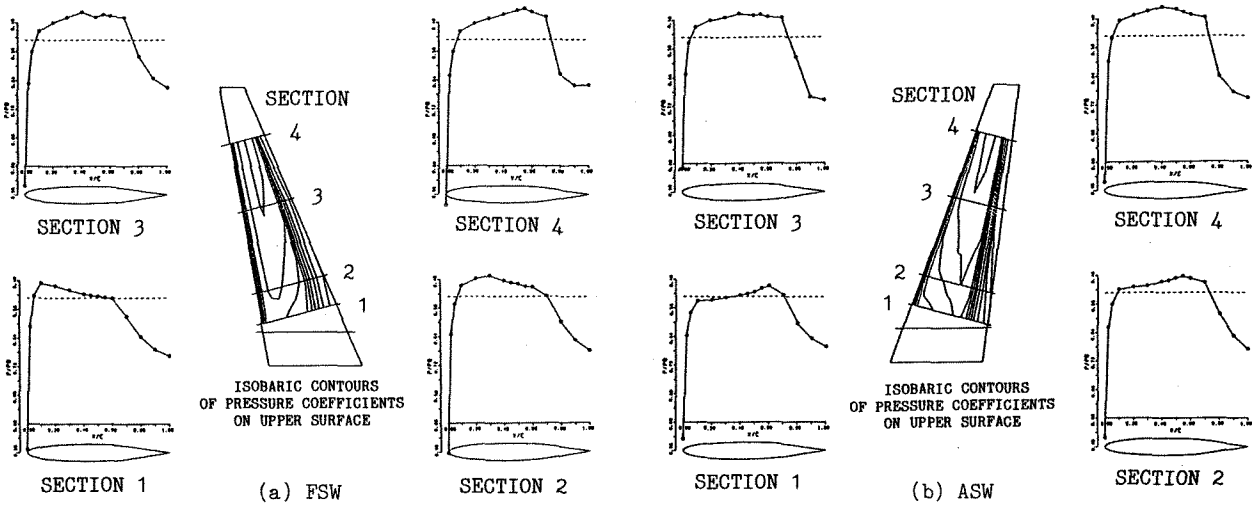

Fig. 8. Pressure Distributions at Four Sections And Isobaric Contours of Pressure Coefficients on Upper Surface

(Mach number = 0.83, attack angle = 0°)

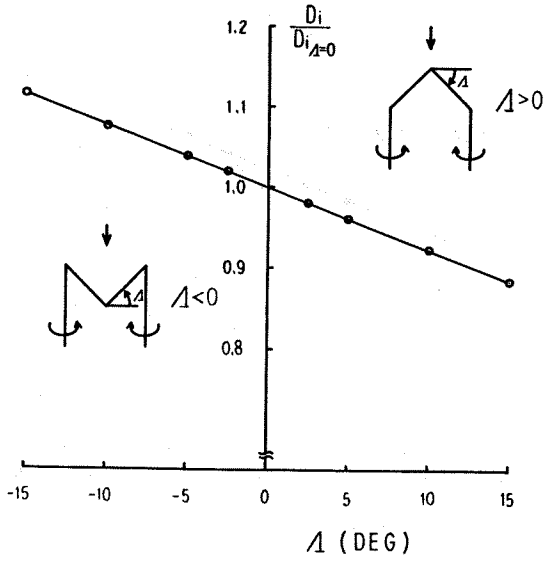

Fig. 10. Sweep Effect on Induced Drag

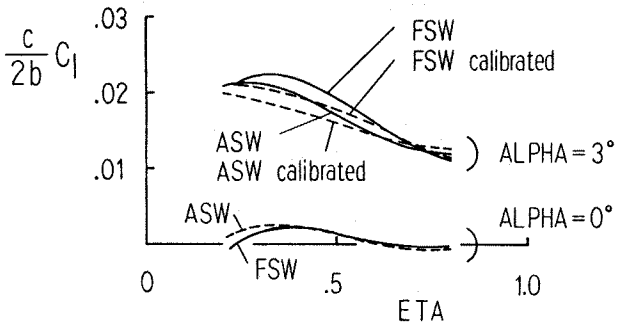

Fig. 11. Spanwise Load Distributions at Mach Number 0.7
'Calibrated' data is obtained by data at Attack Angle 0° Subtracted from Data at Attack Angle 3°.

assumptions, nevertheless, we can see clearly how induced drag is affected by wing sweep direction. Experimental data also shows that induced drag of FSW is greater (Fig. 4).

Though lift coefficient as a whole is equal zero, there exists a spanwise section-lift distribution (Fig. 11). This is due to an error of producing. These distributions of circulation are obtained by interpolation of measured pressure distributions. As shown in Fig. 11, wing load of ASW at the tip becomes larger than that of FSW at Mach number 0.7 and attack angle 3°. This is because outboard induced velocity of ASW is smaller than that of FSW. Therefore one can easily suppose that further increase of attack angle will cause the flow separation at the tip first, that is, tip stall. This is why ASW usually have to be designed with wash-out.

At higher lift coefficients, M_{DD} of ASW is greater than that of FSW (Fig. 7). Pressure distribution at Mach number 0.79 and attack angle 3°, which is just before M_{DD}, is shown in Fig. 12. One can see that at the root of FSW the flow is accelerated quickly and forms shock wave. And what is worse, it has almost right angle to the flow. On the contrary, shock wave does not exist inboard for ASW. The strength of wave drag is much greater inboard than outboard for FSW (Fig.13). This figure shows that this time M_{DD} of FSW is lower than that of ASW and drag divergence occurs due to the inboard shock wave for FSW.

As for lift divergence Mach number (M_{LD}), any clear distinct between FSW and ASW could not be recognized (Fig. 14). Fig. 15 shows how the trailing edge pressure coefficients decrease according with Mach number. For both wings the outboard trailing edge pressure begins to decrease at the same time as Mach number exceeds M_{LD}. This figure shows how the flow separates. These

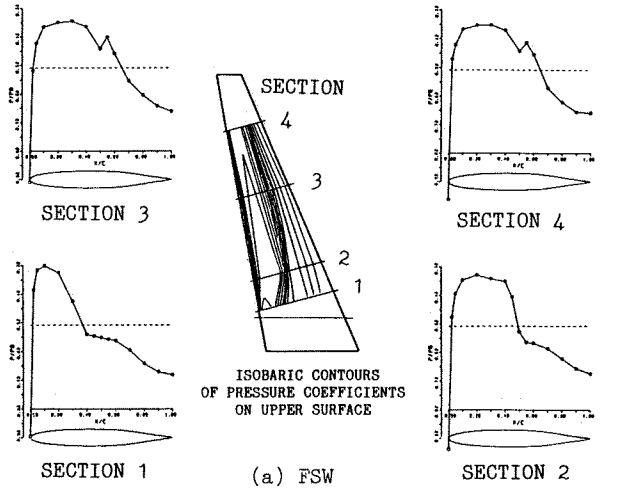

Fig. 12. Pressure Distributions at Four Sections And Isobaric Contours of Pressure Coefficients on Upper Surface
(Mach number = 0.79, attack angle = 3°)

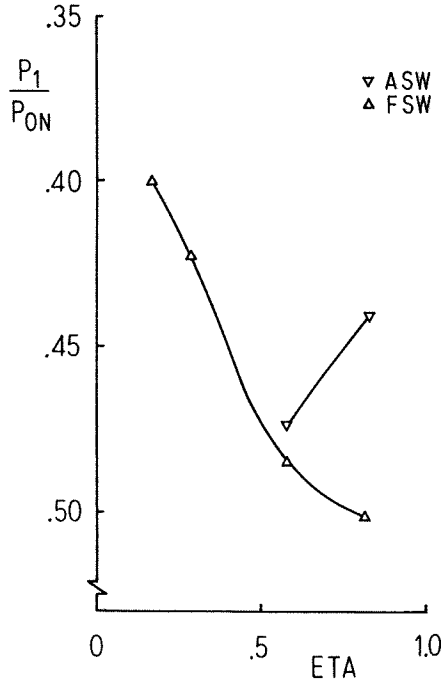

Fig. 13. Spanwise Distributions of P_1/P_{ON}

(Mach number = 0.79, attack angle = 3°)

separations are due to compressibility, that is, shock wave. At M_{LD}, FSW has stronger shock wave inboard than outboard. As shock wave at the root is located forward, the separated flow just downstream of the shock wave could not reach the trailing edge and forms the separation bubble. Therefore the downstream pressure recovery is good. However, as shock wave at the tip, which is weaker than at the root, is at rearward position, the separated flow reaches the trailing edge and this makes the trailing pressure decrease. This fact also indicates that lift divergence occurs due to outboard separation for both wings.

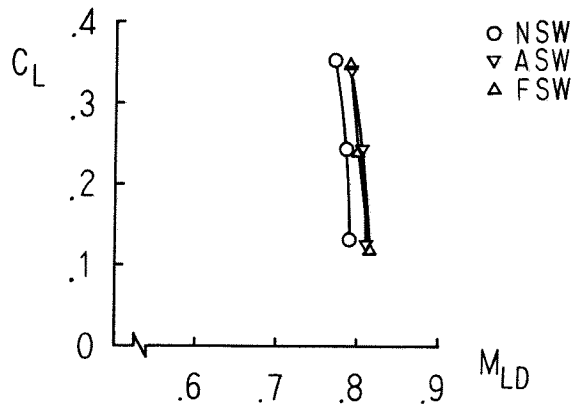

Fig. 14. Lift Divergence Mach Numbers

4. CONCLUSIONS

An experimental investigation has been carried out in transonic flow to make the fundamental characteristics of forward-swept wing clear. It is shown that induced drag of forward-swept wing is larger than estimated with the existing theory. And compared with structurally equivalent aft-swept wing, forward-swept wing has following fundamental aerodynamic characteristics.

At zero lift condition,

1) wave drag is smaller because shock-wave sweep is smaller
2) the boundary layer is supposed to be laminar in larger region because form drag is much smaller.

With non-zero lift coefficients,

1) induced drag is fundamentally larger because the edge of trailing vortices is located forward.

And a problem that should be solved for forward-swept wing is presented, namely, the airfoil at the root should be designed carefully so that strong shock wave does not occur.

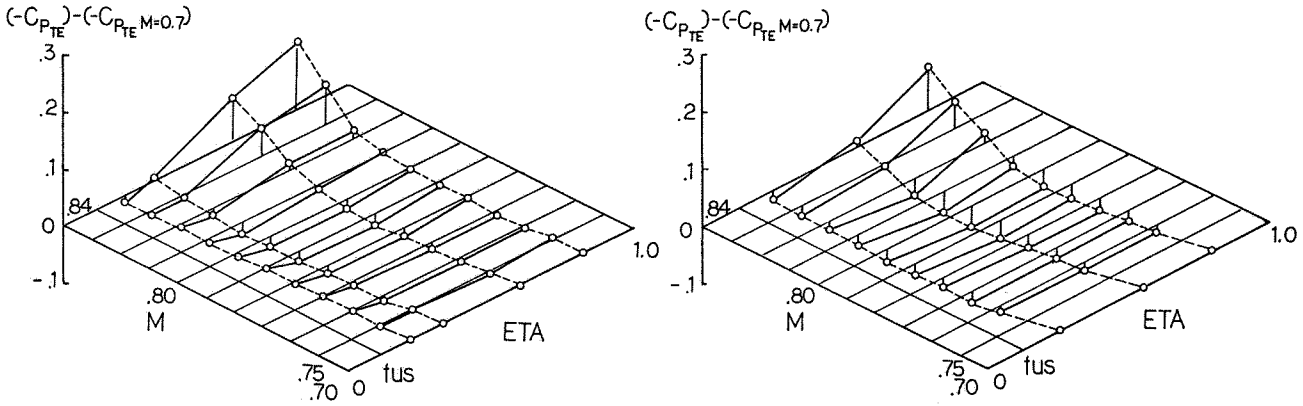

Fig. 15. Variation of Trailing-Edge Pressure Distributions with Mach Number at Attack Angle of 2°

REFERENCES

1. KRONE, N.J.Jr., "Divergence Elimination with Advanced Composites", AIAA-75-1009 (1975)

2. KRONE, N.J.Jr., "Forward Swept Wing Flight Demonstrator", AIAA-80-1882 (1980)

3. UHUAD, G.C., WEEKS, T.M., and LARGE, R., "Wind Tunnel Investigation of the Transonic Aerodynamic Characteristics of Forward Swept Wings", J. Aircraft, 20, 3, March (1983)

4. TRUCKENBRODT, E., "How to Improve The Performance of Transport Aircraft by Variation of Wing Aspect-Ratio And Twist", ICAS-80-0.1 (1980)

5. MUNK, M.M., "Isoperimetrische Aufgaben aus der Theorie des Fluges", Dissertation, Gottingen Univ. (1919)

6. ISHIGURO, T., "Numerical Analysis of Inviscid Flows about Wing-Fuselage Combinations II. Development of Full Potential Flow Code YOKUDO-P", NAL TR-881 (1985)

7. PAISLEY, D.J., and POLL, D.I.A., "Laminar Flow And Transition on Swept Wings", Proceedings International conference FORWARD SWEPT WINGS, Univ. of Bristol (1982)